

## Towards high-resolution land elastic FWI?

J. Cao<sup>1</sup>, A. Sedova<sup>1</sup>, M. Reinier<sup>1</sup>, D. Donno<sup>1</sup>, G. Lambare<sup>1</sup>

<sup>1</sup> Viridien

### Summary

---

The benefits of moving from acoustic full-waveform inversion (FWI) to elastic FWI have now been demonstrated in case of complex geology in the offshore contexts. With onshore data, there are also high expectations about the potential benefits of moving to elastic FWI. This is of particular interest in the Middle East, where the near-surface heterogeneities consist of alternating layers of shales and carbonates, resulting in very strong velocity contrasts that create strong elastic effects including energetic and dispersive surface waves, converted waves and numerous multiples. With this work we contribute to the debate on the advantages of transitioning from acoustic to elastic land FWI. We have investigated here the potential improvements that high-resolution elastic land FWI can bring compared to acoustic land FWI, by adding multi-parameter joint inversion of P- and S-wave velocity models and a selective attenuation of the surface waves to our elastic land FWI toolbox.

## Towards high-resolution land elastic FWI?

### Introduction

The benefits of moving from acoustic full-waveform inversion (FWI) to elastic FWI have been demonstrated recently in the case of complex geology of the offshore environments (Wu et al., 2022). For onshore data, acoustic FWI often struggles with near-surface heterogeneities. Therefore, there are high expectations about the potential benefits of moving to elastic FWI, since elastic modelling engine can better simulate the near-surface wave propagation. This is of particular interest in the Middle East, where the near-surface heterogeneities consist of alternating layers of shales and carbonates, resulting in significant velocity contrasts. They create strong elastic effects including energetic and dispersive surface waves, P-to-S or S-to-P converted body waves and numerous multiples. The first applications of elastic FWI to Middle East land data (e.g., Plessix and Pérez-Solano, 2015; Bharti et al., 2016; Adwani et al., 2022; Leblanc et al., 2022; Sedova et al., 2024) revealed that a simultaneous extraction of the information from all wave types was challenging. Hence, suitable model- or data-driven strategies are essential for mitigating parameter cross-talk and energy differences among different wave-types (e.g., where highly energetic ground roll covers or masks a large part of reflected and converted waves). To improve land imaging with elastic FWI, we consider the following strategies:

- 1) Joint P- and S-wave velocity model ( $V_p$  and  $V_s$ ) inversion for addressing the parameter cross-talk issue,
- 2) Selective attenuation of the surface waves during elastic wave modelling.

The latter aims to retrieve the information from reflections that are hidden behind the energetic surface waves, which enables the application of high-resolution FWI Imaging technique (Guo et al., 2025). The effectiveness of these two strategies is assessed on a 2D synthetic case study and further illustrated on a field data example from the Middle East.

### Elastic FWI strategy for land data

#### *Joint inversion of $V_p$ and $V_s$*

Unlike acoustic FWI, elastic FWI is driven by two velocity parameters,  $V_p$  and  $V_s$ . Compared to marine applications, the stronger elastic effects of land data require a multi-parameter joint inversion of  $V_p$  and  $V_s$  models (Pérez-Solano and Plessix, 2019; Adwani et al., 2022). To illustrate the impact of a multi-versus a mono-parameter inversion, we show a synthetic example inspired from the geology of the Middle East (Figure 1b). We compare the results of 18 Hz elastic FWI mono-parameter  $V_p$  inversion ( $V_s$  is updated assuming a fixed but erroneous  $V_p/V_s$  ratio) with multi-parameter joint ( $V_p, V_s$ ) inversion. Both approaches start with the same initial models: the initial  $V_p$  is shown in Figure 1a, and the initial  $V_s$  is built by applying a 1D linear decreasing trend of  $V_p/V_s$  from 2.5 to 2.0.

Figures 1c and 1d show the  $V_p$  models obtained with the mono-parameter and multi-parameter inversions, respectively. It can be observed that, due to the added degree of freedom, multi-parameter joint ( $V_p, V_s$ ) inversion contributes to mitigating the  $V_s$  wavenumber leakage in the  $V_p$  update and stabilizing the  $V_p$  update free from high-wavenumber contamination. This is visible in the 1D view of the  $V_p$  profile in Figure 1e. In addition, enabling multi-parameter joint ( $V_p, V_s$ ) inversion allows for better interpretation of the recorded S waves independent of the P waves in this context, where the S-wave energy is significant in the observed data. Consequently, both  $V_p$  and  $V_s$  updates benefit from the multi-parameter joint inversion and produce models much closer to the true ones (Figure 1e).

#### *Surface-wave attenuation in elastic FWI*

To increase the resolution of the inverted velocity model, it is essential to include high-frequency reflected waves (Guo et al., 2025) in the inversion. However, the complex near surface with fast S-wave velocities, commonly in the Middle East region, results in energetic surface waves that cover or mask a large part of reflected waves. This issue has been discussed in Plessix and Pérez-Solano (2015), who proposed a modification of the free-surface boundary condition aimed at not producing surface waves. However, although this strategy effectively eliminates the surface waves, it also alters the phase and

amplitude of the reflections of the body waves at the free surface (Leblanc et al., 2022). Here we propose a new approach that attenuates the surface waves on-the-fly during elastic modelling in the elastic FWI, while preserving the other body wave behaviours (as shown in Figure 2).

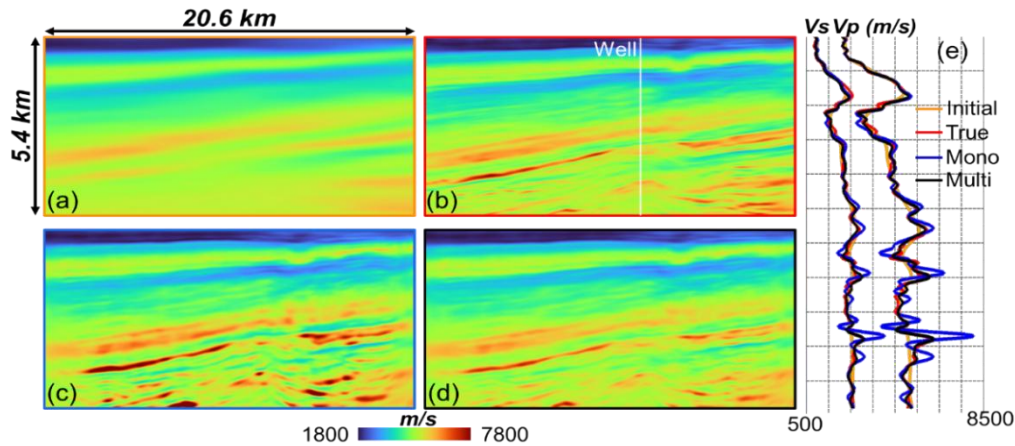


**Figure 1.** Velocity model illustrations of the synthetic study. (a) Initial  $V_p$ , (b) true  $V_p$ , (c) inverted  $V_p$  from mono-parameter elastic FWI (with fixed erroneous  $V_p/V_s$  ratio), (d) inverted  $V_p$  from multi-parameter joint ( $V_p, V_s$ ) elastic FWI, and (e) 1D profile comparison of all the  $V_p$  models and corresponding  $V_s$  models at the well location indicated by the white line in (b).

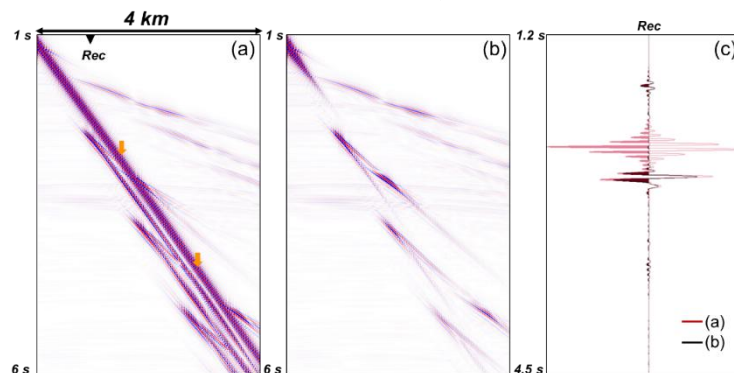


**Figure 2.** The modelled shot gathers obtained from elastic FWI: (a) without, and (b) with the on-the-fly surface-wave attenuation technique. The energetic and highly dispersive surface waves indicated by the orange arrows in (a) are no longer modelled in (b), and the trace comparison at receiver location (Rec) shows the body waves are well preserved in (c).

## Real-data application

The real data example presented here comes from the Middle East, in a test area of approximately 400 km<sup>2</sup> characterized by complex geological structures. The geology in this region is favourable to the application of acoustic FWI, particularly when careful data pre-conditioning is applied (Guo et al., 2025). The application of elastic FWI in this context allows for refining the  $V_p$  model and providing additional information through the  $V_s$  model update. In the velocity model building workflow, we implemented the two strategies highlighted above, i.e., joint ( $V_p, V_s$ ) inversion and on-the-fly surface-wave attenuation in the elastic modelling. Figure 3 presents the comparisons of acoustic and elastic FWI results. Both are obtained through the same two-step inversion scheme. First, we perform FWI up to 8 Hz using an inner mute to remove the near-offset contributions to concentrate on establishing the low-wavenumber components of the updated models from the diving and P-S converted waves. Figures 3a and 3d illustrate the data fit comparison of vertical component of particle velocity ( $V_z$ ) after this step. The elastic FWI (Figure 3d) interprets a larger portion of the observed data including the slow converted waves (indicated by the white arrows) that cannot be predicted by the acoustic engine. During the second step we invert from 8 to 15 Hz, including reflections at near offsets to enhance the resolution of the resulting velocity model for deriving the FWI Images. At this step, we employ the on-the-fly surface-wave attenuation technique. The resulting velocity models (Figures 3b and 3e) show that the

elastic FWI at 15 Hz provides a more accurate near-surface velocity model, characterized by improved geological conformity to the shallow layer (indicated by the blue arrows in Figures 3b and 3e) and better handling of the velocity reversals as delineated by the orange boxes. The elastic FWI Image shows improved resolution, especially in the near surface and above 1 km depth, and reduced multiple and converted wave contamination (indicated by the orange arrows in Figures 3c and 3f).

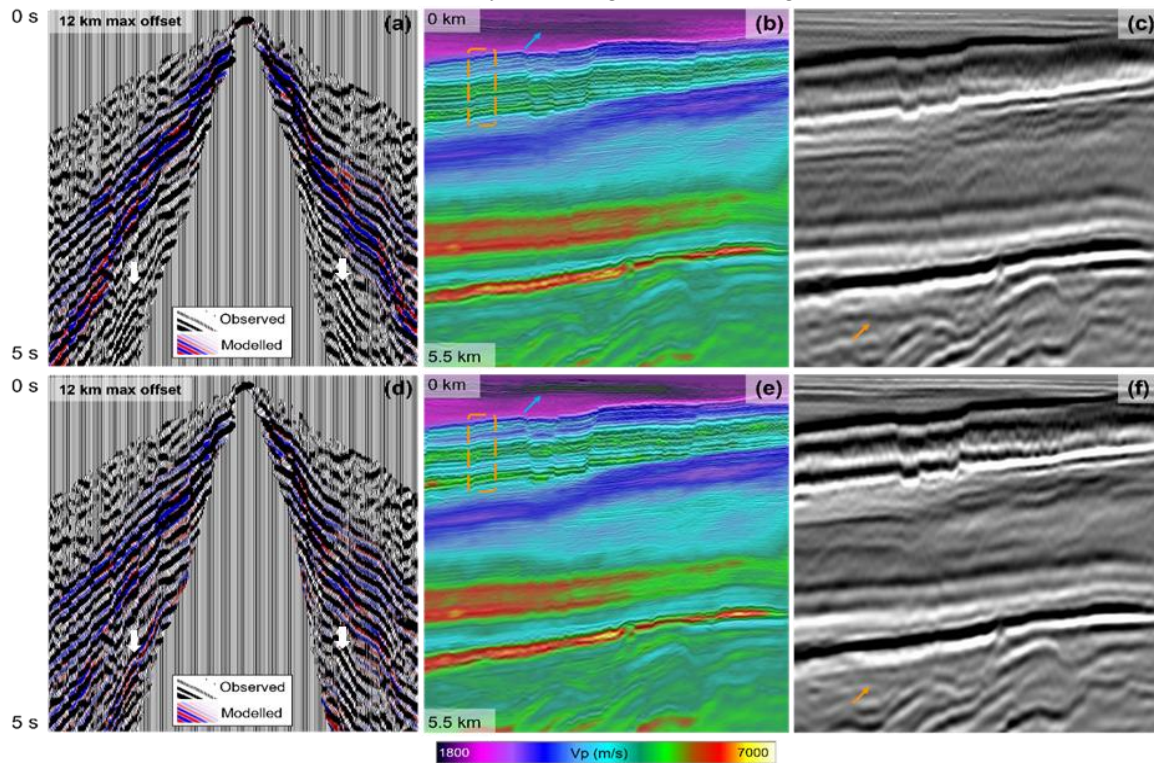


**Figure 3.** (a) Inversion result comparison at 15 Hz between acoustic FWI (a, b and c) and multi-parameter joint ( $V_p, V_s$ ) elastic FWI (d, e and f). From left to right:  $V_z$  component data-fits at 8 Hz between the observed and modelled data, P-wave velocity models ( $V_p$ ) and FWI Images derived from the 15 Hz  $V_p$  models.

Figure 4 provides a closer look at the shallow section, highlighting the accurate reconstruction of the  $V_p$  velocity reversal in the layers between 1 and 2 km of depth using 15 Hz elastic FWI. The joint ( $V_p, V_s$ ) inversion enables an accurate construction of the  $V_s$  model, which subsequently enhances the  $V_p$  model update. The impact of attenuating the surface waves while preserving the reflected waves in the elastic FWI is demonstrated in Figure 5. The reflections at near offsets and hidden behind the surface waves are usable in elastic FWI, improving the elastic FWI Image resolution (Figure 5b) compared to the result obtained when simply muting out the surface waves (Figure 5a).

## Conclusions

Investigating land elastic FWI for better handling the challenges of complex geologies is of highly scientific importance. We presented here two important components in the elastic FWI toolbox: 1) multi-parameter joint ( $V_p, V_s$ ) inversion enabling more accurate construction of  $V_p$  and  $V_s$  models in the areas characterised by strong elastic effects; 2) an effective attenuation of the surface waves in the data and in the elastic wave modelling to take advantage of high-frequency reflected waves for high-resolution FWI imaging. By showing the imaging improvements brought by this method, our work contributes to the debate on the advantages of moving from acoustic FWI to elastic FWI on land.

## Acknowledgements

We thank Occidental Petroleum (Oxy) and the Ministry of Energy and Minerals of the Sultanate of Oman for permission to publish the data examples, and Viridien for permission to publish this work.

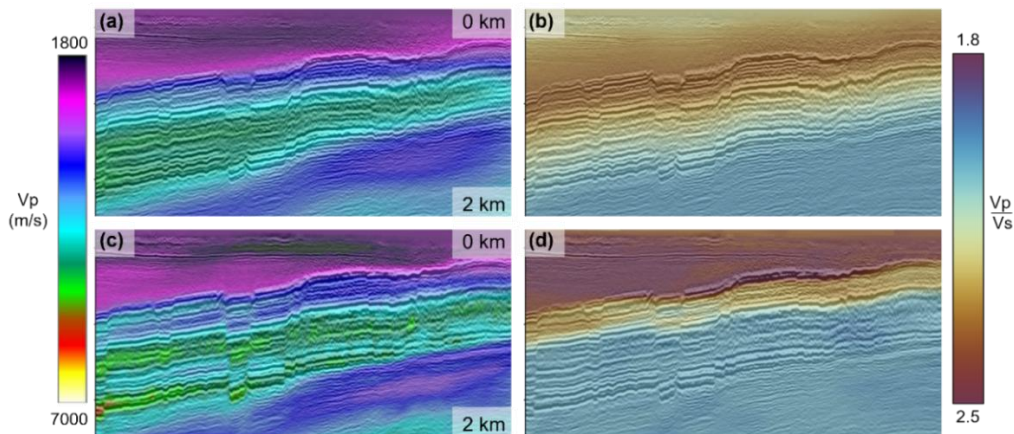


**Figure 4.** Illustration of models of: (a) initial  $V_p$  and (b) initial  $V_p/V_s$  ratio, and (c) updated  $V_p$  and (d) updated  $V_p/V_s$  ratio from the multi-parameter joint ( $V_p$ ,  $V_s$ ) elastic FWI.

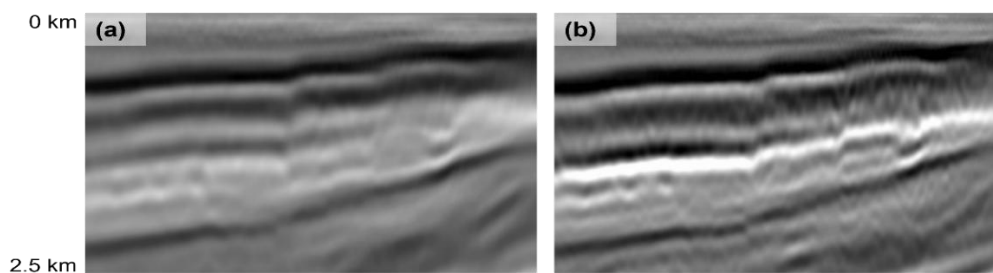


**Figure 5.** Comparison of FWI Images obtained from the same elastic FWI configuration, except for: (a) not using, and (b) using the on-the-fly surface wave attenuation technique, which allows avoiding the inner data mute and exploiting reflections during elastic FWI.

## References

- Adwani, A., Danilouchkine, M., Al-Siyabi, Q., Al-Droushi, O., ten Kroode, F., Plessix, R.E. and Ernst, F. [2022] Onshore model building using elastic full-waveform inversion on surface and body waves: A case study from Sultanate of Oman. *Geophysics*, **87**(6), R413-R424.
- Bharti, S., Stopin, A., Pérez-Solano, C.A., Plessix, R.E., Lutz, J., Al-Qadeeri, B., Dashti, Q., Narhari, S. and Olusegun, K. [2016] Application of an anisotropic elastic multiparameter waveform inversion on a land data set from north Kuwait. *86<sup>th</sup> SEG Annual International Meeting*, Expanded Abstracts, 1201-1205.
- Guo, Y., Aziz, A., Sedova, A., Reinier, M., Donno, D., Lambaré, G. and Carotti, D. [2025] Unlocking onshore imaging challenges with FWI: case studies from the Sultanate of Oman. *The Leading Edge*, **44**(1), 306-316.
- Leblanc, O., Sedova, A., Lambaré, G., Allemand, T., Hermant, O., Carotti, D., Donno, D. and Masmoudi, N. [2022] Elastic land full-waveform inversion in the Middle East: method and applications. *83rd EAGE Annual Conference & Exhibition*, Extended Abstracts.
- Pérez-Solano, C. and Plessix, R.-É. [2019] Velocity-model building with enhanced shallow resolution using elastic waveform inversion - An example from onshore Oman. *Geophysics*, **84**(6), R977-R988.
- Plessix, R.É. and Pérez Solano, C.A. [2015] Modified surface boundary conditions for elastic waveform inversion of low-frequency wide-angle active land seismic data. *Geophysical Journal International*, **201**(3), 1324-1334.
- Sedova, A., Leblanc, O., Reinier, M., Donno, D., Lambaré, G. and Carotti, D. [2024] Near-surface characterization by elastic full-waveform inversion of surface waves. *85th EAGE Annual Conference & Exhibition*, Extended Abstracts, 1-5.
- Wu, Z., Wei, Z., Zhang, Z., Mei, J., Huang, R. and Wang, P. [2022] Elastic FWI for large impedance contrasts. *2<sup>nd</sup> International Meeting for Applied Geoscience & Energy*, Expanded Abstracts, 3686-3690.